

부분적으로 가려진 물체 인식을 위한 어닐드 홉필드 네트워크

Annealed Hopfield Neural Network for Recognizing Partially Occluded Objects

윤석훈(Suk-Hun Yoon)*

초 록

컴퓨터 비전 적용 분야에서 부분적으로 가려진 물체 인식의 필요성은 증가하고 있다. 물체를 확인하고 위치를 지정하는 데에 물체가 가려진 것은 심각한 문제를 야기한다. 이 논문은 여행자 소지 수하물에서 위험 물건을 발견하기 위하여 어닐드 홉필드 네트워크를 제안한다. 어닐드 홉필드 네트워크는 하이브리드 홉필드 네트워크와 어닐링 이론에 기초한 확정적 근사방법이다. 하이브리드 홉필드 네트워크는 위험 물체의 이미지에서 발췌한 경계 점들과 코너 점들을 이용한다. 또한 어닐드 홉필드 네트워크의 런타임을 줄이기 위해 임계 온도를 조사하였다. 어닐드 홉필드 네트워크와 하이브리드 홉필드 네트워크의 성능을 비교하기 위하여 광범위한 컴퓨터 실험이 실행되었다.

ABSTRACT

The need for recognition of partially occluded objects is increasing in the area of computer vision applications. Occlusion causes significant problems in identifying and locating an object. In this paper, an annealed Hopfield network (AHN) is proposed for detecting threat objects in passengers' check-in baggage. AHN is a deterministic approximation that is based on the hybrid Hopfield network (HHN) and annealing theory. AHN uses boundary features composed of boundary points and corner points which are extracted from input images of threat objects. The critical temperature also is examined to reduce the run time of AHN. Extensive computational experiments have been conducted to compare the performance of the AHN with that of the HHN.

키워드 : 홉필드 네트워크, 부분적으로 가려진 물체, 어닐링, 인식
Hopfield Network, Partially Occluded Objects, Annealing, Recognition

* Associate Professor, Department of Industrial and Information Systems Engineering, Soongsil University
(yoonsu@ssu.ac.kr)

Received: 2021-04-29, Review completed: 2021-05-10, Accepted: 2021-05-16

1. Introduction

Detecting objects and estimating their pose are critical problems and challenging tasks due to noise, low resolution, occlusion, clutter, or other interference factors in many computer vision application [4, 14]. In particular, a key problem for computer vision systems is how to deal with partial occlusion. In many real-world images, objects are often surrounded and partially occluded by each other [3]. The large variability of occluders in terms of their shape, appearance and position introduces an exponential complexity in the data distribution that is infeasible to be exhaustively represented in finite training data [11].

With the rapid development of the computer industry, neural networks have been applied to various areas such as control, computer vision and image processing, classification, and optimization [1, 5, 17]. Hopfield neural network is a fully connected feedback neural network. Thus, the output signal for each neuron is fed back to itself through other neurons, making Hopfield neural networks feedback neural networks.

This paper addresses the recognition problem of partially occluded objects. Hybrid Hopfield neural network (HHN) has provided reliable solutions and reduced computational time in detecting partially occluded objects. HHN estimated the behavior of neurons based on the distinguishable value of a connectivity matrix. However, HHN does not guarantee a

near optimal solution because it depends on initial conditions. While HHN generally produced some useful results, it also suffered from significant drawbacks. These include many spurious stable points in the case of the traveling salesman problem.

In this paper, an annealed Hopfield network (AHN), which is based on neural networks and annealing is proposed to recognize the partially occluded objects. AHN uses corner points extracted from the boundary of an image by using a constraint regularization technique and a mean field annealing method [15]. Following the literature review in the next section, AHN is developed in section 3. In addition, a critical point range of AHN is estimated to try to reduce the run time. In section 4, the experimental results of HHN and AHN are provided and analyzed using a t-test. Finally, a summary of main results and conclusions are provided in section 5.

2. Literature Review

2.1 Hopfield Neural Network

Hopfield neural networks can be classified by discrete Hopfield network (DHN) and continuous Hopfield network (CHN) [6, 7, 8, 9]. Hopfield constructs neural network by connecting many simple processing elements (neurons) to each other. Two variables (current state and output) generally describe an

i th neuron. The current state and the output are generally denoted by u_i and V_i , respectively. A simple nondecreasing monotonic output function $g(u_i)$ usually relates the output to the state. This function is designed to limit the possible values of V_i to the range -1 to $+1$. In other words, $g(u_i)$ is frequently a step function (in the case of DHN) or a sigmoid function (in CHN). When neuron i has a connection made to it from neuron j , the strength of connection is defined as C_{ij} . The input of each neuron comes from two sources: external inputs (I_i) and inputs from other neurons. The total input to neuron i is then [9].

$$H_i = \sum_{j \neq i} C_{ij} V_j + I_i \quad (1)$$

Each neuron changes the value of its output or leaves it fixed according to a threshold rule with thresholds U_i [9]

$$\begin{aligned} V_i &\rightarrow V_i^0 \quad \text{if} \quad \sum_{j \neq i} C_{ij} V_j + I_i < U_i \\ &\rightarrow V_i^1 \quad \text{if} \quad \sum_{j \neq i} C_{ij} V_j + I_i > U_i \end{aligned} \quad (2)$$

Hopfield constructed an energy function [9]

$$\begin{aligned} E = & -\frac{1}{2} \sum_{i \neq j} \sum C_{ij} V_i V_j \\ & - \sum_i I_i V_i + \sum_i U_i V_i \end{aligned} \quad (3)$$

where $V_i = 0, 1$

In this paper, the states of the neurons are expressed by the vector u , the outputs by the vector v , the connection strengths by the matrix C , and the external inputs by the vector i^b .

The discrete version where the value of the state vector at time step $n+1$ is related to the neuron output vector at time step n by the equation [2]

$$u^{(n+1)} = C v^{(n)} + i^b \quad (4)$$

The motion of the state of a system which has N neurons in a state space describes the computation that the set of neurons is performing. Each neuron i readjusts its state randomly in time but with a mean attempt rate W . The value of output changes can be expanded to more than two-dimensional network as follows

$$\begin{aligned} v &\rightarrow v^0 \quad \text{if} \quad C v^{(n)} + i^b < u \\ &\rightarrow v^1 \quad \text{if} \quad C v^{(n)} + i^b > u \end{aligned} \quad (5)$$

The CHN describes the behavior of the network by a following differential equation [2]

$$\frac{du}{dt} = -\frac{u}{\lambda} + C v + i^b \quad (6)$$

and CHN has output function $g(u_i)$ as a sigmoid function

$$g(u^i) = \frac{1}{1 + \exp(-2u^i/\theta)} \quad (7)$$

$$u^i = g^{-1}(v)$$

If the elements of u are updated asynchronously and the connection matrix C is symmetric, then Hopfield shows that the DHN has a Liapunov function of the form [2]

$$E = -\frac{1}{2} v^t C v - (i^b)^t v \quad (8)$$

where the contents of v are 0, 1.

For CHN with either synchronous or asynchronous update, the following Liapunov function exist

$$E = -\frac{1}{2}v^t C v - (i^b)^t v + \beta \quad (9)$$

$$\text{where } \beta = \sum_i \sum_k \int_0^{v_{ik}} g^{-1}(V) dV$$

Further, in high-gain limit (i.e., $u^0 \rightarrow 0$ and $g(x)$ asymptotically approaches a step function), the Liapunov function of CHN is approximately the same as that of DHN.

2.2 Hybrid Hopfield Network

Hybrid Hopfield network (HHN) constructs a two-dimensional array for a matching problem. HHN approaches a matching problem through minimizing the following energy function [10]

$$\begin{aligned} E = & -\frac{A}{2} \sum_i \sum_k \sum_j \sum_l C_{ikjl} V_{ik} V_{jl} \quad (10) \\ & + \frac{B_1}{2} \sum_i \sum_k \sum_{(l \neq k)} V_{ik} V_{il} \\ & + \frac{B_2}{2} \sum_k \sum_i \sum_{i \neq j} V_{ik} V_{jk} \end{aligned}$$

The columns of an array represent nodes of an object model, and the rows represent nodes of an input object. Therefore, the state of each neuron represents measure of matching between two nodes from each graph. V_{ik} is the binary variable which converges to 1 if the i th node in the input image matches the k th node in the object model; otherwise, it converges to 0. The first term in Eq. (10) is a

compatibility constraint. The normalizing local and relational features which have different measures gives the tolerance for ambiguity of the features. The last two terms enforce the uniqueness constraint so that each node in the object model eventually matches only one node in the input image and the summation of the outputs of the neurons in each row or column equals 1. In addition, normalizing local and relational features which have different measures gives a tolerance for ambiguity of the features as follows

$$\begin{aligned} C_{ijkl} = & W_1 \times F(f_i, f_k) + W_2 \times F(f_j, f_l) \quad (11) \\ & + W_3 \times F(r_{ij}, r_{kl}) \end{aligned}$$

The fuzzy function F has a value of 1 for a positive support and -1 for a negative support. The value of $F(x, y)$ is defined such that if the absolute value of the difference between x and y is less than a threshold θ , then $F(x, y)$ is set to 1, otherwise $F(x, y)$ is set to -1. The values of W 's reflect the importance of each term. The sum of the weights is 1. The f_i and f_j represents local features with angles between corners and r_{ij} represents relational features with distances between corners. Hopfield proved that the energy function is a Liapunov function. Thus, the energy function converges to a local minimum when the states of neurons converge to stable states [13].

HHN combines the benefits of DHN and CHN. HHN uses output of DHN as inputs of CHN since the configuration of the outputs of DHN is very close to the stable state of

the desired output of CHN. After running DHN, HHN adjusts the output of DHN by an analyzing procedure based upon CHN theory.

3. Annealed Hopfield Network

In recognizing target objects by boundary-based approaches, corner points are important since the information of the shape is concentrated at the points having high curvatures. From the corner points, two useful features can be extracted which are local features (an angle between neighboring corners) and relational features (distances between the corners). These features which are invariant under translational and rotational changes, are used for the robust shape description of the boundary. Corner points are usually detected in a curvature function space by capturing the points whose curvature values are above a certain threshold value. A graph can be constructed for an object model using corner points as nodes of the graph. For the matching process, a similar graph is constructed for the input image which may consist of one or several overlapped objects.

A motion equation is shown in Eq. (6) with the sigmoid function g . The energy function of the matching problem is organized as Eq. (8). The output of each neuron for the matching problem has the value of 0 or 1 to represent measure of similarity. Output of each

neuron will be called a spin for the annealing approach. It was assumed that the spin interactions C_{ikjl} are symmetric and have no self-interaction (i.e., $C_{ikik} = 0$). The state space of each spin is

$$s_{ik} \in \{0, 1\} \quad \text{for } 1 \leq i, k \leq N \quad (12)$$

In simulated annealing, random perturbations move the system towards its thermal equilibrium at the current temperature. Assuming that all the spins are at equilibrium, one can determine the i th spin average $\langle s_{ik} \rangle$ from the Boltzmann distribution and the change in the average system energy as s_{ik} flips from 0 to 1. Let

$$\begin{aligned} H_0 &= \langle H(s) \rangle \Big|_{s_{ik}=0} \\ H_1 &= \langle H(s) \rangle \Big|_{s_{ik}=1} \end{aligned} \quad (13)$$

Then the equilibrium value of $\langle s_{ik} \rangle$ is calculated as below [16]

$$\begin{aligned} \langle s_{ik} \rangle &= Pr\{s_{ik}=0\} \times 0 + Pr\{s_{ik}=1\} \times 1 \quad (14) \\ &= \frac{\exp\left(-\frac{H_1}{T}\right)}{\exp\left(-\frac{H_0}{T}\right) + \exp\left(-\frac{H_1}{T}\right)} \\ &= \left\{ 1 + \exp\left[-\frac{H_0 - H_1}{T}\right] \right\}^{-1} \\ &= \left\{ 1 + \exp\left[-\frac{u_{ik}}{T}\right] \right\}^{-1} \end{aligned}$$

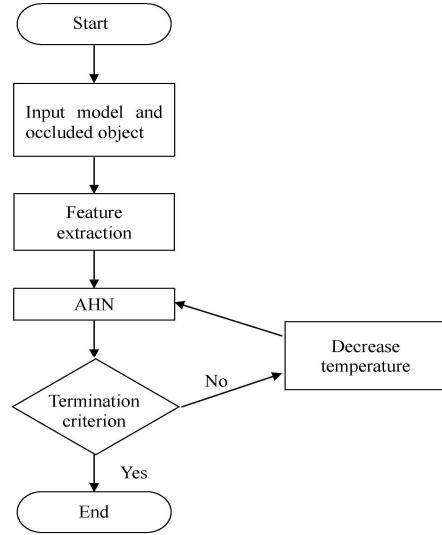
The u_{ik} is defined to represent the quantity $H_0 - H_1$, which is the mean or effective field experienced by the ik^{th} spin. It generally is difficult to compute u_{ik} for large N

$$\begin{aligned} \langle H(s) \rangle &= \left\langle \sum_i \sum_j \sum_k \sum_k C_{ijkl} s_{ik} s_{jl} \right. & (15) \\ &\quad \left. + \sum_i \sum_k I_{ik} s_{ik} \right\rangle \\ &= \sum_i \sum_j \sum_k \sum_k C_{ijkl} \langle s_{ik} s_{jl} \rangle \\ &\quad + \sum_i \sum_k I_{ik} \langle s_{ik} \rangle \end{aligned}$$

Since s_{ik} and s_{jl} are not independent, their expected values are not separable in the above equation. However, when the number of interacting spins is large enough that the effect of any single spin on any other spins is very small in comparison to the total field, then the mean field approximation can be as follows

$$\begin{aligned} \langle H(s) \rangle &= \sum_i \sum_j \sum_k \sum_k C_{ijkl} \langle s_{ik} \rangle \langle s_{jl} \rangle & (16) \\ &\quad + \sum_i \sum_k I_{ik} \langle s_{ik} \rangle \end{aligned}$$

The Eq. (14) and Eq. (16) has the same structure as Eq. (7) and Eq. (8). In addition, random perturbation to move the system towards its thermal equilibrium in simulated annealing is the same as updating rule of the Hopfield network. The only difference is that λ in eq. (7) is replaced with temperature T . It means that given T , flow to thermal equilibrium in the annealing process is the same as the flow of Hopfield network given λ . Therefore, if we find the stable points of states by slowly lowering λ from the high value, then global solutions or near global solution of the network will be found without initial restriction. <Figure 1> represents the flowchart of the AHN.



<Figure 1> Flow Chart of the Algorithm

An initial temperature for the annealed networks significantly affects the quality of final solutions. Starting at too high temperature is time-consuming since no progress is made until the critical temperature (T_c) is reached. On the contrary, starting at too low temperature quickly can force the system into a poor solution. Van Den Bout et al. [16] used a normalization technique to improve solutions of TSP. However, the technique was hard to implement since it was not a natural flow in biological neural networks (or the analog Hopfield network model). Instead, in this paper the sigmoid function is used to derive the critical temperature. The spin perturbations near T_c are small enough so that all the spins remain near their high temperature average of $1/N$. With this assumption, the effect that mean field changes have on the spins are found from the sigmoid function in Eq. (14) to be

$$\frac{\partial s_{ik}}{\partial u_{ik}} = \frac{N-1}{N^2 T} \quad (17)$$

From Eq. (6),

$$\frac{\partial u_{ik}}{\partial s_{jl}} = \begin{cases} 0, & ik = jl \\ C_{ikjl}, & ik \neq jl \end{cases} \quad (18)$$

The change of s_{ik} (Δs_{ik}) cause the change of inputs of the other neurons Δu_{jl} as follows

$$\begin{aligned} \Delta u_{jl} &= \frac{\partial u_{jl}}{\partial s_{ik}} \Delta s_{ik} + \sum_{jl \neq ik} \frac{\partial u_{jl}}{\partial s_{jl}} \Delta s_{jl} \\ &= C_{ikjl} \Delta s_{ik} \end{aligned} \quad (19)$$

The change of s_{jl} (Δs_{jl}) from the change of u_{jl} is

$$\Delta s_{jl} = \frac{\partial s_{jl}}{\partial u_{jl}} \Delta u_{jl} = \frac{N-1}{N^2 T} C_{ikjl} \Delta s_{ik} \quad (20)$$

From the change of s_{jl} (Δs_{jl}), the new input of ik th neuron (Δu_{ik}^b) is

$$\begin{aligned} \Delta u_{ik}^b &= \frac{\partial u_{ik}}{\partial s_{ik}} \Delta s_{ik} + \sum_{jl \neq ik} \frac{\partial u_{ik}}{\partial s_{jl}} \Delta s_{jl} \\ &= \sum_{jl \neq ik} C_{ikjl} \frac{N-1}{N^2 T} C_{ikjl} \Delta s_{ik} \\ &= \Delta s_{ik} \frac{N-1}{N^2 T} \sum_{jl \neq ik} C_{ikjl}^2 \end{aligned} \quad (21)$$

Therefore, the new perturbation Δs_{ik}^b is derived from the Eq. (21)

$$\begin{aligned} \Delta s_{ik}^b &= \frac{\partial s_{ik}}{\partial u_{ik}} \Delta u_{ik} \\ &= \frac{N-1}{N^2 T} \frac{N-1}{N^2 T} \Delta s_{ik} \sum_{ik \neq jl} C_{ikjl}^2 \end{aligned} \quad (22)$$

In fact, Hopfield network in the object matching problem is a fully connected network and the flow of the output change of neurons is very complicated. The result assumes that output changes of all the other neurons caused by the change of the ik th neuron (Δs_{ik}) are fed back to the ik th neuron and force the change of the ik th neuron to be accelerated when the temperature is near T_c . Therefore, the effect of other neuron outputs is ignored to simplify this problem. Let an average of connection strength be w . At the critical temperature, the spin perturbation must persist so that $\Delta s_{ik}^b = \Delta s_{ik}$. As a result,

$$\begin{aligned} \Delta s_{ik}^b &= \frac{(N-1)^2}{N^4 T^2} \Delta s_{ik} N^2 w^2 \\ &= \frac{(N-1)^2}{N^2 T^2} \Delta s_{ik} w^2 \end{aligned} \quad (23)$$

At $T = T_c$, $\Delta s_{ik}^b = \Delta s_{ik}$

$$T_c = \frac{N-1}{N} |w| \cong |w| \quad (24)$$

for $N \gg 1$.

4. Experimental Results

Eight guns (models) and five tools were used to make seventy-seven occluded objects for the matching procedure. The tools were a hammer, a screwdriver, nuts, pliers and spanners (wrenches). Model images were

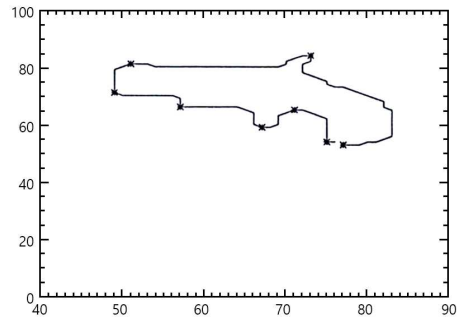
obtained by a camera and a commercially available digitizer. Boundaries of the images were obtained by the chain code method. The number of boundary points for the models ranged from 225 to 514. After extracting the boundary, corner points (nodes) were extracted by using the optimal boundary smoothing method based on the regularization technique [15]. The number of nodes in the models ranged from 7 to 14. From each node, features were extracted: an angle as a local feature and the distance between nodes as a relational feature. Occluded images were obtained through the same procedure as models. The number of boundary points for the occluded images ranged from 421 to 816 and the number of nodes ranged from 7 to 29. <Figure 2> showed the boundaries and corner points of a sample model and occluded object. Occlusion rate (OR) was computed as follows:

$$OR = \frac{\text{No. of nodes of the model occluded by another object}}{\text{No. of nodes of the model}} \quad (25)$$

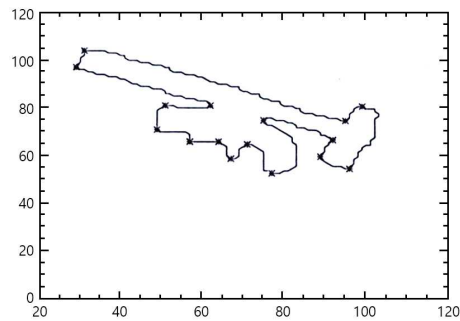
To compare the performance of HHN and AHN, matching score (MS) was computed as follows:

$$OR = \frac{\text{No. of exactly matched nodes}}{\text{No. of matchable nodes}} \quad (26)$$

In <Figure 2(a)>, the number of the corner points in the model were 8. Among them, 2



(a) Model

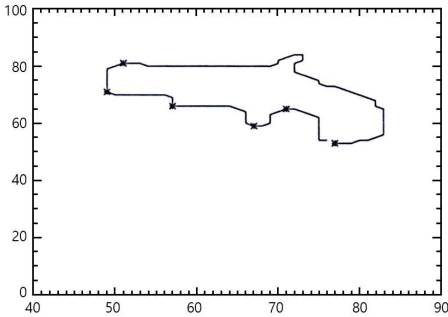


(b) Occluded object

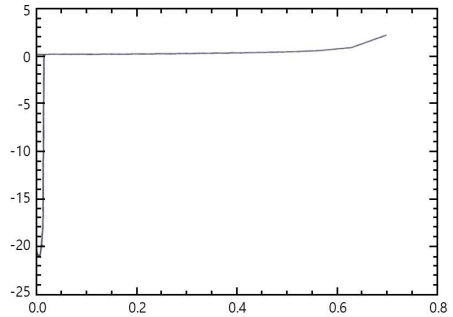
<Figure 2> Boundaries and Corner Points of the Model and the Occluded Object

corner points were covered in the occluded object as shown in <Figure 2(b)> and hence OR was 0.25.

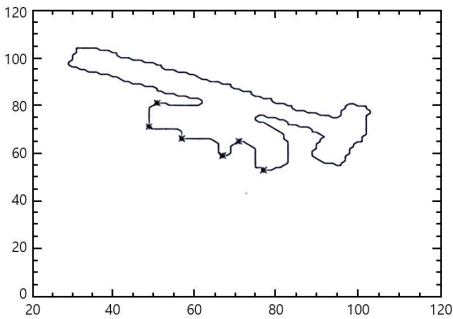
<Figure 3> showed the extracted corner points of the model and the occluded model after the matching procedure. After occlusion, 2 corner points of the model in <Figure 3(a)> were covered by a hammer and only 6 points could be matched (that is, no. of matchable nodes was 6). As shown in <Figure 3(b)>, 6 points of the model were exactly matched with the corresponding points in the occluded object and as a result MS was 1.



(a) Model after matching



<Figure 4> Energy Graph



(b) Occluded object after matching

<Figure 3> Matched Nodes in the Model and the Occluded Object

<Table 1> Results of the Experiments (Matching Score)

Occlusion Rate	HHN	AHN
0~9%	0.93	1.00
10~19%	0.90	1.00
20~29%	0.80	0.95
30~39%	0.71	0.86
40~49%	0.84	0.95
50~59%	0.42	0.71
over 60 %	0	0.33
Total	0.72	0.88

The results of the HHN and the AHN were shown in <Table 1>. AHN gave perfect MS for slightly occluded objects up to 20% OR. Even for half occluded objects, AHN provided

more than 90% MS. Without heavily occluded objects, MS of the AHN were 96% on the average. From the results of slightly occluded objects, it was shown that AHN provided near optimum solutions for the partially occluded object recognition.

AHN decreased the temperature by some rate (5% in the experiment) to escape local minima and find a global minimum. However, it would take a long time to reach the optimum if an initial temperature were too high. Thus, estimation of the initial temperature reasonably high to reach the optimum called the critical temperature (T_c) would be required. As shown in <Figure 4>, energy dropped precipitously around the critical temperature. The experimental result of T_c was 0.02 to 0.1 while the estimate of T_c was 0.7. This discrepancy might result from the smaller number of neurons than we assumed.

To compare the performance of AHN and HHN, a t -test was used since the sampling size was large for the population to follow normal distribution [12]. The complete t -test

was summarized in <Table 2>. Using a significant level $\alpha = 0.05$ in the t -test, it was concluded that AHN provided better matching score than HHN.

<Table 2> Results of t -Test

	AHN	HHN
Mean	0.876623	0.722468
Variance	0.091654	0.186324
Observations	77	77
Pearson Correlation	0.565203	
Hypothesized Mean Difference	0	
df	76	
t Stat	3.748057	
$P(T \leq t)$ one-tail	0.000173	
t Critical one-tail	1.665151	
$P(T \leq t)$ two-tail	0.000345	
t Critical two-tail	1.991675	

5. Summary and Conclusions

This paper has addressed the recognition problem of threat objects under partial occlusion. For the recognition problems, HHN has provided good results but severely depended on initial conditions. In this paper, AHN which incorporates Hopfield network and the annealing theory was developed to avoid the drawback of the HHN. Experiments show that AHN outperforms HHN regardless of the occlusion rates. For slightly occluded objects, AHN provided near optimum solutions. The critical temperature was estimated and used as an initial temperature for the annealing pro-

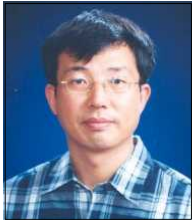
cess to shorten the run-time of the algorithm. AHN is a robust approach for solving two-dimensional detection problems under occlusion. A three-dimensional recognition problem of partially occluded objects would be the extension of this research.

References

- [1] Agliari, E., Barra, A., and Notarnicola, M., "The relativistic Hopfield network: rigorous results," *Journal of Mathematical Physics*, Vol. 60, No. 3, pp. 1-11, 2019.
- [2] Aiyer, S. V. B., Niranjana, M., and Fallside, F., "A Theoretical Investigation into the Performance of the Hopfield Model," *IEEE Transactions on Neural Networks*, Vol. 1, No. 2, pp. 204-215, 1990.
- [3] Cen, F. and Wang, G., "Boosting Occluded Image Classification via Subspace Decomposition-Based Estimation of Deep Features," *IEEE Transactions on Cybernetics*, Vol. 50, No. 7, pp. 3409-3422, 2020.
- [4] Cong, Y., Tian, D., Feng, Y., Fan, B. and Yu, H., "Speedup 3-D texture-less object recognition against self-occlusion for intelligent manufacturing," *IEEE Transactions on Cybernetics*, Vol. 49, No. 11, pp. 3887-3897, 2019.
- [5] de Castro, F. Z. and Valle, M. E., "A broad class of discrete-time hypercomplex-valued Hopfield neural networks," *Neural Net-*

- works, Vol. 122, pp. 54-67, 2020.
- [6] Hopfield, J. J. and Tank, D. W., "‘Neural’ Computation of Decisions in Optimization Problems," *Biological Cybernetics*, Vol. 52, pp. 141-152, 1985.
- [7] Hopfield, J. J. and Tank, D. W., "Computing with neural circuits: a model," *Science*, Vol. 233, pp. 625-633, 1986.
- [8] Hopfield, J. J., "Neural networks and physical systems with emergent collective computational abilities," *Proceedings of the National Academy of Sciences of the United States of America*, Vol. 79, pp. 2554-2558, 1982.
- [9] Hopfield, J.J ., "Neurons with graded response have collective computational properties like those of two-state neurons," *Proceedings of the National Academy of Sciences of the United States of America*, pp. 3088-3092, 1984.
- [10] Kim, J. H., Yoon, S. H., Kim, Y. H., Park, E. H., and Ntuen et al., "Efficient matching algorithm by a hybrid Hopfield network for object recognition," *Proc. SPIE 1709, Applications of Artificial Neural Networks III*, Orlando, FL, September 16, 1992.
- [11] Kortylewski, A., Liu, Q., Wang, A., Sun, Y., and Yuille, "A., Compositional convolutional neural networks: a robust and interpretable model for object recognition under occlusion," *International Journal of Computer Vision*, Vol. 129, pp. 736-760, 2021.
- [12] Montgomery, D. C., *Design and Analysis of Experiments (10th Ed.)*, Wiley, New York, 2020.
- [13] Nasrabadi, N.M. and Li, W., "Object recognition by a Hopfield neural network," *IEEE Transactions on Systems, Man, and Cybernetics*, Vol. 21, No. 6, pp. 1523-1535, 1991.
- [14] Priya, L. and Anand, S., "Object recognition and 3D reconstruction of occluded objects using binocular stereo," *Cluster Computing*, Vol. 21, pp. 29-38, 2018.
- [15] Sohn, K. Alexander, W. E., Kim, J. H., and Snyder, W. E., "A constrained regularization approach to robust corner detection," *IEEE Transactions on System, Man, and Cybernetics*, Vol. 24, No. 5, pp. 820-828, 1994.
- [16] van den Bout, D. E. and Miller III, T.K ., "Graph partitioning using annealed neural networks," *International 1989 Joint Conference on Neural Networks*, Washington DC, USA, pp. 521-528.
- [17] Wang, X.-Y. and Li, Z.-M., "A color image encryption algorithm based on Hopfield chaotic neural network," *Optics and Lasers in Engineering*, Vol. 115, pp. 107-118, 2019.

저 자 소 개



윤석훈

1988년

1995년

2002년

2002년~현재

관심분야

(E-mail: yoon@ssu.ac.kr)

서울대학교 산업공학과 (학사)

NC A&T State University (석사)

Pennsylvania State University (박사)

승실대학교 산업정보시스템공학과 부교수

최적화, 메타휴리스틱, 스케줄링